

See discussions, stats, and author profiles for this publication at: <https://www.researchgate.net/publication/263263615>

Stable Performance of Ni Catalysts in the Dry Reforming of Methane at High Temperatures for the Efficient Conversion of CO₂ into Syngas

ARTICLE *in* CHEMCATCHEM · JANUARY 2014

Impact Factor: 4.56 · DOI: 10.1002/cctc.201300699

CITATIONS

15

READS

25

7 AUTHORS, INCLUDING:



[Andrey Tarasov](#)

Fritz Haber Institute of the Max Planck Soci...

12 PUBLICATIONS 54 CITATIONS

SEE PROFILE



[Malte Behrens](#)

University of Duisburg-Essen

125 PUBLICATIONS 1,610 CITATIONS

SEE PROFILE

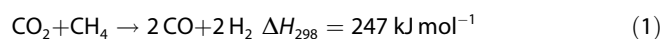
Stable Performance of Ni Catalysts in the Dry Reforming of Methane at High Temperatures for the Efficient Conversion of CO₂ into Syngas

Katharina Mette,^[a] Stefanie Kühl,^[a] Hendrik Düdler,^[b] Kevin Kähler,^[b] Andrey Tarasov,^[a] Martin Muhler,^{*[b]} and Malte Behrens^{*[a]}

The catalytic performance of a Ni/MgAlO_x catalyst was investigated in the high temperature CO₂ reforming of CH₄. The catalyst was developed using a Ni, Mg, Al hydrotalcite-like precursor obtained by co-precipitation. Despite the high Ni loading of 55 wt%, the synthesized Ni/MgAlO_x catalyst possessed a thermally stable microstructure up to 900 °C with Ni nanoparticles of 9 nm. This stability is attributed to the embedding nature of the oxide matrix, and allows increasing the reaction

temperature without losing active Ni surface area. To evaluate the effect of the reaction temperature on the reforming performance and the coking behavior, two different reaction temperatures (800 and 900 °C) were investigated. At both temperatures the prepared catalyst showed high rates of CH₄ consumption. The higher temperature promotes the stability of the catalyst performance due to mitigation of the carbon formation.

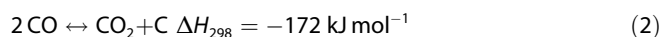
The efficient conversion of CO₂ into various chemicals and fuels is a prospective building block for the more sustainable use of our global resources.^[1] Among the various strategies that have been proposed for converting CO₂ into higher-energy intermediates,^[2] processes that employ heterogeneous catalysis are of special interest, because they are scalable, based on a mature and flexible technology that has already been applied in the chemical industry, and can be integrated into existing value chains.^[3] The dry reforming of methane (DRM) with carbon dioxide is an interesting method for converting these two greenhouse gases into CO/H₂ mixtures [Eq. (1)]. This reaction opens the door to utilizing anthropogenic CO₂, which is obtained from, for example, oxy-fuel-combustion processes, in the well-established downstream chemistry of syngas to afford MeOH and other base chemicals or fuels through Fischer–Tropsch synthesis.



The highly endothermic DRM reaction has long been studied as a potential alternative for the steam reforming of methane

and several comprehensive reviews have been published on this topic.^[4–6] It is well-known that Ru, Rh, and Pt catalysts are very active in this reaction. Active base metals—and Ni in particular—suffer from fast deactivation by coking.^[7,8] However, from an economic point of view, Ni-based catalysts are more suitable for commercial applications than noble-metal ones. Thus, a current challenge is to find a noble-metal-free catalyst that is resistant towards coking.^[9] Promising approaches in the literature include the poisoning of coke-forming sites by sulfur,^[10] variation of the support,^[11] in particular through the application of Lewis-basic materials,^[12] the addition of alkaline or alkaline-earth oxides as promoters,^[13–14] and the incorporation of Ni into a perovskite framework.^[15]


It has been shown that the deposition of carbon over Ni at 700 °C and over Rh at 750 °C originates from the exothermic Boudouard reaction [Eq. (2)] and not primarily from methane decomposition [Eq. (3)].^[16,17]



Thus, the process temperature is an important parameter in the DRM reaction.^[4] Considering the thermodynamics of the desired endothermic DRM and of the undesired exothermic Boudouard reaction, a promising way of suppressing coking would be to perform the DRM reaction at high temperatures.^[18] Typically, 750 °C is an upper limit in many literature reports. In addition, the thermodynamic yields of CO and H₂ would increase at higher temperatures. Following this concept, the primary challenge in making the Ni particles kinetically more resistant to coking involves making a large Ni surface area thermally stable against sintering at more elevated temperatures. Herein, we report the synthesis, characterization and

[a] K. Mette, Dr. S. Kühl, Dr. A. Tarasov, Dr. M. Behrens
Department of Inorganic Chemistry
Fritz-Haber-Institut der Max-Planck-Gesellschaft
Faradayweg 4-6, 14195 Berlin (Germany)
Fax: (+49) 030-8413-4405
E-mail: behrens@fhi-berlin.mpg.de

[b] H. Düdler, Dr. K. Kähler, Prof. Dr. M. Muhler
Laboratory of Industrial Chemistry
Ruhr-University Bochum
Universitätsstr. 150, 44801 Bochum (Germany)
Fax: (+49) 0234-32-14115
E-mail: muhler@techchem.rub.de

 Supporting information for this article, including further experimental details, is available on the WWW under <http://dx.doi.org/10.1002/cctc.201300699>.

catalytic performance of a Ni-rich bulk catalyst that shows sufficient thermal stability of its microstructure.

Our synthetic approach to stabilizing Ni nanoparticles at high temperatures was to incorporate them into a stable oxide matrix, a concept that has previously been applied to Ni-containing perovskites^[15] and spinels.^[19] We attempted to achieve strong interfacial interactions between the metal and the oxide by a stabilizing partial embedding of the Ni particles through the formation of both catalyst components from a single phase precursor with a mixed cationic lattice and decomposable anions. This concept was previously applied to Cu-based catalysts for MeOH synthesis, in which Cu,Zn,Al hydrotalcites were developed as promising catalyst-precursor materials.^[22] The resulting catalysts are characterized by a homogeneous metal distribution and very small Cu particles that were embedded and, therefore, stabilized in an amorphous ZnAl_2O_4 matrix.

Following this concept, we chose a hydrotalcite-like (htl) precursor with the nominal composition $\text{Ni}_x\text{Mg}_{0.67-x}\text{Al}_{0.33}(\text{OH})_2(\text{CO}_3)_{0.17} \cdot m\text{H}_2\text{O}$ ($x=0.5$). This precursor compound could be easily prepared in its phase-pure form by pH-controlled co-precipitation (see the Supporting Information, Figure S1). The application of htl precursors for the preparation of Ni catalysts has been studied before by several groups for the steam and dry reforming of methane. For instance, Takehira and co-workers^[21–26] and Perez-Lopez et al.^[27] presented different synthetic approaches to htl-derived Ni/MgO/ Al_2O_3 catalysts, with Ni content ranging from 22 to 55 mol%, and investigated these materials in the DRM. Moderate coking levels between 500 and 700 °C were reported for a Ni/Mg/Al molar composition of 55:11:33. The high Ni content of 50 mol% (metal base) in our precursor corresponded to a Ni loading of 55 wt% in the final catalyst. This rather high value was chosen to exploit the advantage of higher loadings of cheap and abundant base-metal catalysts. The 1:2 ratio of Mg to Al was expected to lead to spinel formation, MgAl_2O_4 , which is a sintering-stable ceramic compound. Indeed, beneficial effects on the coking behavior of Ni catalysts have been reported on alumina, magnesia, and spinel supports.^[28] First, we will focus on the synthesis and thermal stability of the htl-derived 55 wt% Ni/Mg Al_2O_4 catalyst and then consider the catalytic properties in the DRM at high temperatures and the characterization of the spent samples will be reported.

XRD analysis of the co-precipitated precursor confirmed the htl structure of the precursor and did not indicate the presence of any other crystalline phases (Figure 1a). SEM analysis revealed the typical platelet-like morphology of htl compounds, with a lateral size of up to approximately 200 nm and a thickness in the low-nm range (Figure 1d). The BET surface area of the precursor material was relatively high ($131 \text{ m}^2 \text{ g}^{-1}$). Upon calcination, the htl structure decomposed and the precursor underwent a weight loss of 38% (up to 1000 °C), which was already close to completion at 600 °C (for the TGA curve, see the Supporting Information, Figure S2). The XRD patterns of samples that were calcined at different temperatures are shown in Figure 1b. At 350 and 600 °C, only broad modulations of the background were observed at the peak positions

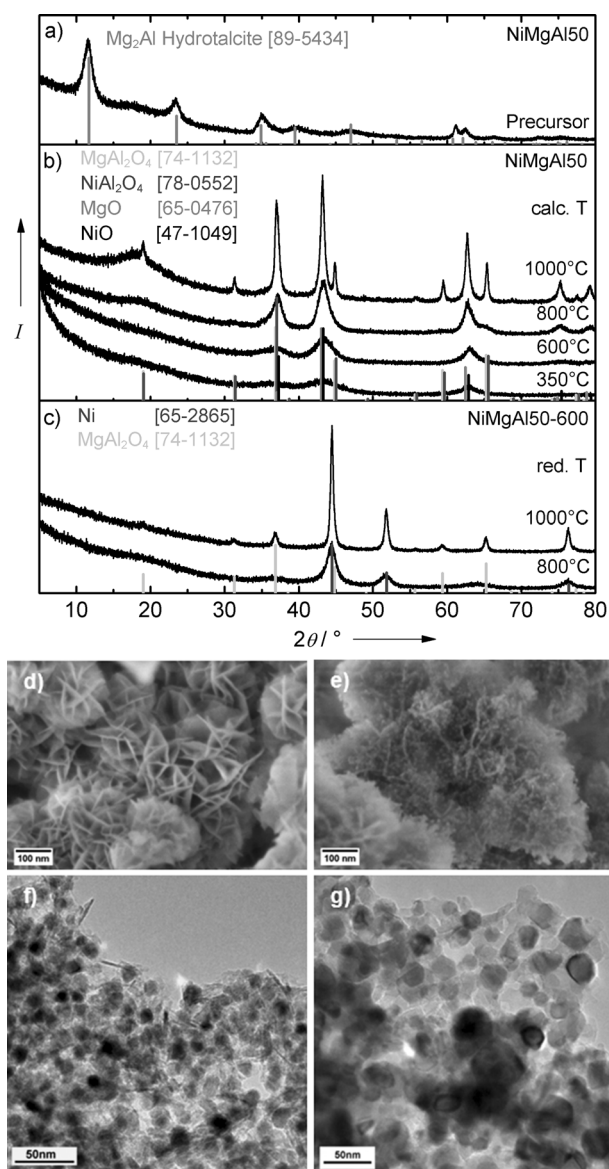


Figure 1. XRD patterns of a) the htl precursor; b) the products that were obtained at different calcination temperatures; c) samples that were calcined at 600 °C after reduction at 800 and 1000 °C; d) SEM images of the precursor material; and e) the catalyst after reduction at 800 °C. TEM micrographs of the fresh Ni/Mg Al_2O_4 catalyst after reduction at f) 800 °C and g) 1000 °C.

of a rock-salt-type phase (NiO or MgO). At 800 °C, crystallization had progressed further and the first indications of a crystalline spinel phase were detected. After calcination at 1000 °C, the XRD pattern showed a mixture of rock-salt- and spinel-type phases, as expected for the decomposition of a htl compound.^[29,30] Owing to the similar diffraction patterns of MgO and NiO and of MgAl_2O_4 and NiAl_2O_4 , as well as the possible formation of solid solutions, no detailed phase identification could be performed based on the XRD data, in particular for the poorly crystalline materials that were obtained at lower calcination temperatures. However, after mild calcination at 600 °C, no indication of the segregation of individual species was found by SEM or by local EDX analyses at different locations (see the Supporting Information, Figure S3 and Table S1).

Thus, we conclude that the calcination product that was obtained at 600 °C is an amorphous, fully dehydrated, and carbonate-free mixed Ni/Mg/Al oxide, the homogenous distribution of the metal species of which had been largely conserved during the decomposition of the htl precursor. The surface area has increased to 213 m² g⁻¹, owing to the weight loss and to shrinkage of the platelets.

After reduction of the calcined material in hydrogen at 800 °C (for the TPR curve, see the Supporting Information, Figure S4), SEM analysis revealed that the platelet-like morphology of the htl precursor was still present, thus indicating strong resistivity of the material against sintering at high temperatures (Figure 1 e). In addition, small bright spheres that were homogeneously distributed over the platelets were observed in the micrograph, thus indicating that, upon reduction, nanoscopic segregation of the components had taken place.

Indeed, XRD analysis (Figure 1 c) clearly confirmed the presence of metallic Ni after calcination at 600 °C and subsequent reduction at 800 °C, with a domain size of 4 nm, according to a peak-width analysis. The oxidic component was still only poorly crystalline and no sharp peaks of the spinel could be detected. TEM analysis of individual platelets in the reduced material revealed an average particle size of Ni of about 10 nm (Figure 1 f and the Supporting Information, Figure S5). The discrepancy between the XRD- and TEM-derived size data is thought to be caused by the polycrystalline and defect-rich nature of the embedded particles.^[32] The Ni surface area was determined by hydrogen-pulse chemisorption (see the Supporting Information, Figure S6) to be 22 m² g_{cat}⁻¹ at a BET surface area of 226 m² g⁻¹ after reduction. Interestingly, increasing the reduction temperature to 900 °C did not significantly influence the Ni particle size (see the Supporting Information, Figure S7). This result was even more important because that temperature was far above the Tammann temperature of Nickel ($T_{\text{Tammann Ni}} = 581\text{ °C}^{[33]}$), thus confirming the high thermal stability of this composite material. However, the domain size increased to 7 nm, in good agreement with the TEM analysis of about 9 nm (Table 1 and the Supporting Information, Figure S5), thus suggesting that the effect of temperature was an annealing of the structural defects rather than sintering. Only treatment at 1000 °C led to pronounced sintering of the Ni particles to an average Ni particle size of about 19 nm, according to the TEM analysis (Figure 1 g), and a domain size of about 14 nm, according to the XRD analysis. This process goes hand in hand with the onset of crystallization of the MgAl₂O₄ spinel in the oxide matrix (Figure 1 c). Accordingly, the specific Ni surface area only decreased slightly to 88% by increasing the reduction temperature from 800 to 900 °C and broke down to only 27% at 1000 °C.

In summary, the characterization data show that the synthesis from the htl precursor yields a Ni catalyst that, despite its

Table 1. Physical properties of Ni particles of NiMgAl50-600 after reduction at different temperatures.

T_{red} [°C]	Domain size [nm] ^[a]	Particle size [nm] ^[b]	Particle-size range [nm] ^[b]	Ni surface area [m ² g _{cat} ⁻¹] ^[c]	Ni surface area [m ² g _{Ni} ⁻¹] ^[c]	Dispersion [%] ^[d]	Interface ratio [%] ^[e]
800	4.30 ± 0.20	10.4 ± 1.3	2–21	22	46	6.0	41.3
900	7.35 ± 0.11	8.9 ± 1.6	2–21	19	40	5.3	58.6
1000	14.10 ± 0.20	19.4 ± 2.2	7–44	6	12	1.6	67.8

[a] Volume-weighted column length based on the integral peak breadths fitted using TOPAS^[31]; [b] determined by TEM; [c] determined by H₂-pulse chemisorption; [d] calculated from the H₂-pulse-chemisorption measurements; [e] calculated from the Ni surface area and TEM particle size.

high Ni loading of 55 wt%, possesses a thermally stable microstructure up to 900 °C. This stability is probably attributed to the embedding nature of the still-amorphous oxide matrix that separates the Ni nanoparticles from each other and, therefore, protects them from sintering, thereby resulting in an interface-to-surface ratio of the particles of 41% (for detailed information, see the Supporting Information); even after thermal treatment up to 900 °C, the dispersion of the Ni particles (5–6%, Table 1), as well as the total specific surface area and the exposed specific Ni surface area, was surprisingly high. Thus, these materials are promising catalysts that have the potential to withstand an increase in the reaction temperature of the DRM to study the suppression of coking.

The catalytic activity and stability of the ex-htl catalysts were investigated in a fixed-bed reactor under isothermal DRM conditions. After a reductive pretreatment up to 800 °C, the DRM reaction was performed at 800 °C and 900 °C. At 800 °C, slight deactivation was observed, whereas, at 900 °C, a higher degree of stable conversion was detected (Figure 2). Even in long-

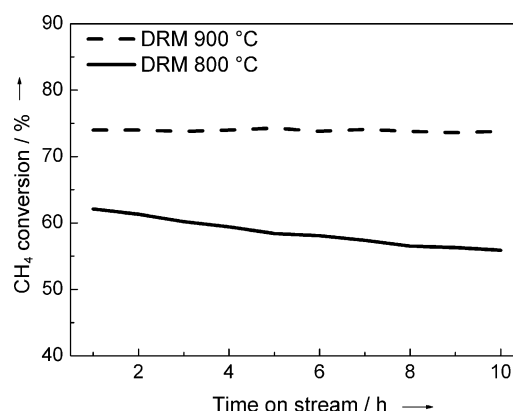


Figure 2. CH₄ conversion as a function of time-on-stream in the DRM at 800 °C and 900 °C using the Ni/MgAlO_x catalyst after reduction up to 800 °C.

term experiments, the catalyst showed a remarkable stable activity at 900 °C, thereby still achieving 94% of the initial conversion of CH₄ after 100 h (see the Supporting Information, Figure S8). This result was attributed to the stabilizing effect of the oxide matrix, which only allowed minor sintering of the active Ni nanoparticles, as confirmed by TEM and XRD.

The integral rates of methane conversion, as determined after 60 min time on stream, were 3.5 × 10⁻³ mol s⁻¹ g_{cat}⁻¹ at 800 °C and 4.2 × 10⁻³ mol s⁻¹ g_{cat}⁻¹ at 900 °C. These values are,

to the best of our knowledge, the highest reported rates for DRM catalysts in the literature.

During a subsequent temperature-programmed oxidation (TPO) experiment, the formation of CO_2 was observed, owing to the presence of carbonaceous deposits. In the TPO profile after DRM at 800°C , two signals at 580°C and 670°C were identified, which afforded an overall amount of $117 \text{ mmol g}_{\text{cat}}^{-1}$ of formed CO_2 . In the DRM at 900°C , the degree of carbon deposition decreased to $54 \text{ mmol g}_{\text{cat}}^{-1}$, including a third carbon species that was detected at 780°C (Figure 3). Once

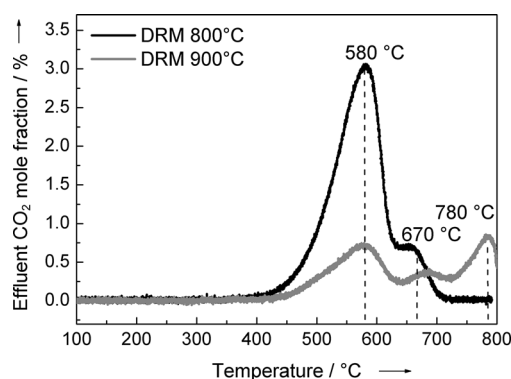


Figure 3. TPO profiles after DRM at 800 and 900°C ($F = 40 \text{ Nml min}^{-1}$, 4.5% O_2/Ar , $\beta = 5 \text{ K min}^{-1}$, $T_{\text{max}} = 800^\circ\text{C}$). Dry-reforming conditions: $T_{\text{oven}} = 800$ or 900°C , $F_{\text{total}} = 240 \text{ Nml min}^{-1}$, 32% $\text{CH}_4/40\% \text{ CO}_2/28\% \text{ Ar}$ (CO_2/CH_4 , 1.25:1).

the carbon deposits had been completely removed by TPO, the initial activity for the DRM was recovered (see the Supporting Information, Figure S9). Thus, the observed deactivation during the DRM at 800°C was predominantly caused by the formation of carbon deposits and not by sintering. In agreement with the TPO results, Raman spectra of spent samples after DRM revealed a lower graphitic content at 800°C (see the Supporting Information, Figure S12). These results indicate that the carbon-formation mechanism is influenced by the reaction temperature. At 800°C , a significant amount of carbon nanotubes (CNTs) is formed, thereby giving rise to the TPO peak at 580°C , whereas, at 900°C , fewer CNTs and a more-stable type of carbon are formed, presumably by pyrolysis of CH_4 [Eq. (3)].

The presence of different amounts and types of carbon in the spent samples was also observed in the TEM analysis of the catalysts after 10 h in an analogous test without a final TPO step. After reaction at 800°C , in addition to a slight sintering of the Ni particles (see the Supporting Information, Figure S10 and Table S2), at least three different carbon species were formed, that is, carbon nanotubes (Figure 4a), graphitic layers (Figure 4c), and carbon onions with the inclusion of Ni particles (Figure 4b). TEM investigation of the catalyst after reaction at 900°C (see the Supporting Information, Figure S11) confirmed the TPO result, because much less carbon was detected. Furthermore, the CNTs were still present but to a much lower extent and they were less well-connected to the catalyst material.

In summary, we have shown that mitigation of the coking problem of noble-metal-free Ni catalysts for the DRM is possi-

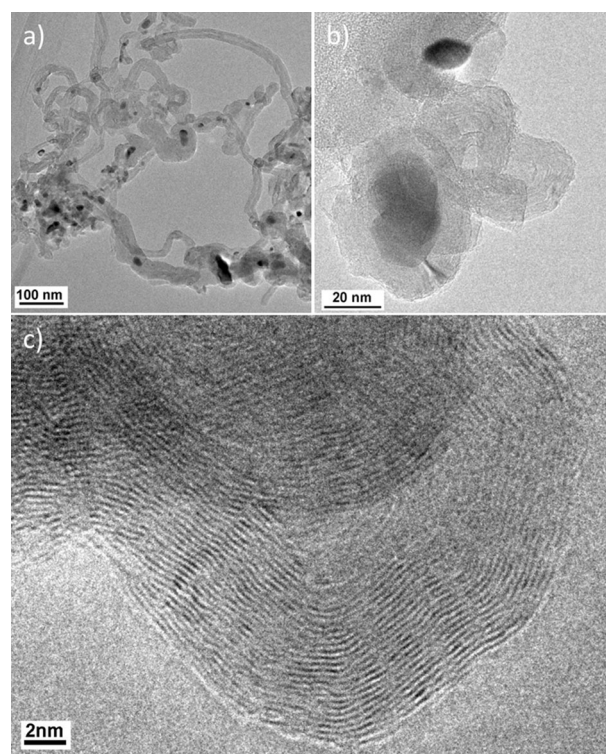


Figure 4. TEM micrographs of the spent sample after the DRM at 800°C for 10 h: a) CNTs that contain Ni particles; b) isolated Ni particles in carbon onions; and c) layers of graphitic carbon.

ble by elevating the operating temperature towards 900°C . This favorable operating window can only be exploited if nanostructured catalysts with sufficient thermal stability are available to survive these harsh conditions. We have reported the synthesis, characterization, and catalytic testing of a highly active and stable Ni/MgAlO_x catalyst that was characterized by small Ni particles, which were partially embedded in an oxide matrix with a high specific Ni and total BET surface area. Despite the high Ni loading of 55 wt%, this catalyst only showed minor sintering at 900°C and performed stably in the DRM over 100 h with an outstanding activity. Compared to the lower reaction temperatures, the major problem of coking was (to a large extent) overcome on this stable Ni catalyst by increasing the reaction temperature to 900°C , which led to the formation of a less-fibrous carbon material.

Experimental Section

The catalysts were prepared by constant pH-controlled co-precipitation in an automated laboratory reactor (Mettler-Toledo Labmax) at 50°C from a 0.6 M aqueous solution of NaOH, a 0.09 M aqueous solution of Na_2CO_3 , and a 0.4 M aqueous solution of the metal nitrate at pH 8.5. The obtained precursor was calcined in air at 600°C for 3 h, thereby yielding almost-amorphous mixed oxides.

For the catalytic experiments, the ex-htl Ni/MgAlO_x catalyst (10 mg, sieve fraction: 250–355 μm) that had been calcined at 600°C prior to the experiment was used in a fixed-bed tubular quartz reactor. The sample was diluted in SiC (490 mg). For the pretreatment, the

catalyst was reduced in 4% H₂/Ar (20 Nmlmin⁻¹). The DRM was performed at 800 or 900 °C in 40% CO₂/32% CH₄/Ar (240 Nmlmin⁻¹) for 10 or 100 h, respectively. Subsequent TPO experiments were performed in 4.5% O₂/Ar (40 Nmlmin⁻¹). Analysis of the gaseous products was performed on a multi-channel gas analyzer (MLT 4, Emerson) with a paramagnetic oxygen detector (Magnos 16, Hartmann & Braun) for the transient experiments and a calibrated GC for the activity tests (Shimadzu GC-14B).

Acknowledgements

The authors thank Robert Schlögl for his support and valuable discussions. The help of Frank Girgsdies and Gisela Weinberg with various characterization techniques is greatly acknowledged. Financial support was provided by the Federal Ministry of Education and Research of Germany (BMBF, FKZ 01RC1006) within the framework of the "CO2RRECT" project.

Keywords: CO₂ conversion · coking · dry reforming of methane · hydrotalcite · Ni nanoparticles

- [1] C. Song, *Catal. Today* **2006**, 115, 2–32.
[2] W. Wang, S. Wang, X. Ma, J. Gong, *Chem. Soc. Rev.* **2011**, 40, 3703–3727.
[3] R. Schlögl, *ChemSusChem* **2010**, 3, 209–222.
[4] M. C. J. Bradford, M. A. Vannice, *Catal. Rev. Sci. Eng.* **1999**, 41, 1–42.
[5] Y. H. Hu, E. Ruckenstein, *Adv. Catal.* **2004**, 48, 297–345.
[6] M.-S. Fan, A. Z. Abdullah, S. Bhatia, *ChemCatChem* **2009**, 1, 192–208.
[7] A. T. Ashcroft, A. K. Cheetham, M. L. H. Green, P. D. F. Vernon, *Nature* **1991**, 352, 225–226.
[8] S. Wang, G. Q. Lu, *Energy Fuels* **1996**, 10, 896–904.
[9] C.-j. Liu, J. Ye, J. Jiang, Y. Pan, *ChemCatChem* **2011**, 3, 529–541.
[10] J. R. Rostrup-Nielsen, *J. Catal.* **1984**, 85, 31–43.
[11] M. C. J. Bradford, M. A. Vannice, *Appl. Catal. A* **1996**, 142, 73–96.
[12] T. Horiuchi, K. Sakuma, T. Fukui, Y. Kubo, T. Osaki, T. Mori, *Appl. Catal. A* **1996**, 144, 111–120.
[13] Z. L. Zhang, X. E. Verykios, *Catal. Today* **1994**, 21, 589–595.
[14] S.-B. Tang, F.-L. Qiu, S.-J. Lu, *Catal. Today* **1995**, 24, 253–255.
[15] V. R. Choudhary, B. S. Uphade, A. A. Belhekar, *J. Catal.* **1996**, 163, 312–318.
[16] H. M. Swaan, V. C. H. Kroll, G. A. Martin, C. Mirodatos, *Catal. Today* **1994**, 21, 571–578.
[17] V. A. Tsipouriari, A. M. Efstathiou, Z. L. Zhang, X. E. Verykios, *Catal. Today* **1994**, 21, 579–587.
[18] J.-W. Snoeck, G. F. Froment, M. Fowles, *Ind. Eng. Chem. Res.* **2002**, 41, 4252–4265.
[19] J. Guo, H. Lou, H. Zhao, D. Chai, X. Zheng, *Appl. Catal. A* **2004**, 273, 75–82.
[20] a) M. Behrens, I. Kasatkin, S. Köhl, G. Weinberg, *Chem. Mater.* **2010**, 22, 386–397; b) S. Köhl, M. Friedrich, M. Armbrüster, M. Behrens, *J. Mater. Chem.* **2012**, 22, 9632–9638.
[21] T. Shishido, M. Sukenobu, H. Morioka, R. Furukawa, H. Shirahase, K. Takehira, *Catal. Lett.* **2001**, 73, 21–26.
[22] K. Takehira, T. Shishido, P. Wang, T. Kosaka, K. Takaki, *Phys. Chem. Chem. Phys.* **2003**, 5, 3801–3810.
[23] K. Takehira, T. Shishido, P. Wang, T. Kosaka, K. Takaki, *J. Catal.* **2004**, 221, 43–54.
[24] A. I. Tsyganok, T. Tsunoda, S. Hamakawa, K. Suzuki, K. Takehira, T. Haya-kawa, *J. Catal.* **2003**, 213, 191–203.
[25] K. Takehira, T. Shishido, D. Shouro, K. Murakami, M. Honda, T. Kawabata, K. Takaki, *Appl. Catal. A* **2005**, 279, 41–51.
[26] K. Takehira, T. Kawabata, T. Shishido, K. Murakami, T. Ohi, D. Shoro, M. Honda, K. Takaki, *J. Catal.* **2005**, 231, 92–104.
[27] O. W. Perez-Lopez, A. Senger, N. R. Marcilio, M. A. Lansarin, *Appl. Catal. A* **2006**, 303, 234–244.
[28] Y.-G. Chen, J. Ren, *Catal. Lett.* **1994**, 29, 39–48.
[29] F. Cavani, F. Trifirò, A. Vaccari, *Catal. Today* **1991**, 11, 173–301.
[30] F. Zhang, X. Xiang, F. Li, X. Duan, *Catal. Surv. Asia* **2008**, 12, 253–265.
[31] TOPAS version 3, copyright 1999, 2000 Bruker AXS2.
[32] J. Sehested, A. Carlsson, T. V. W. Janssens, P. L. Hansen, A. K. Datye, *J. Catal.* **2001**, 197, 200–209.
[33] J. Rostrup-Nielsen, L. J. Christiansen in *Concepts in Syngas Manufacture*, Vol. 10 (Ed.: G. J. Hutchings), Imperial College Press, London, **2011**, pp. 219–227.

Received: August 21, 2013

Published online on October 9, 2013